J Physiol (2003), **549.1**, *pp.* 157–169
DOI: 10.1113/jphysiol.2002.034439

www.jphysiol.org

Chick RGS2L demonstrates concentration-dependent selectivity for pertussis toxin-sensitive and -insensitive pathways that inhibit L-type Ca^{2+} channels

Patrizia Tosetti, Valeria Parente*, Vanni Taglietti*, Kathleen Dunlap and Mauro Toselli*

*Department of Neuroscience, Tufts University School of Medicine, Boston, MA 02111, USA and *Departments of Cellular and Molecular Physiology and Pharmacology, and INFM, University of Pavia, Italy*

In neuronal cells, the influx of Ca^{2+} ions through voltage-dependent L-type calcium (L) channels couples excitation to multiple cellular functions. In addition to voltage, several neurotransmitters, hormones and cytokines regulate L channel gating via binding to G-protein-coupled receptors. Intracellular molecules that modify G-protein activity – such as regulator of G-protein-signalling (RGS) proteins – are therefore potential candidates for regulating Ca^{2+} influx through L channels. Here we show that a novel RGS2 splice variant from chick dorsal root ganglion (DRG) neurons, RGS2L, reduces bradykinin (BK)-mediated inhibition of neuronal L channels and accelerates recovery from inhibition. Chick RGS2 reduces the inhibition mediated by both the pertussis toxin (PTX)-sensitive ($G_{i/o}$-coupled) and the PTX-insensitive (presumably $G_{q/11}$-coupled) pathways. However, we demonstrate for the first time in a living cell that the extent of coupling to each pathway varies with RGS2L concentration. A low concentration of recombinant chick RGS2L (10 nM) preferentially reduces the inhibition mediated by the PTX-insensitive pathway, whereas a 100-fold higher concentration attenuates both PTX-sensitive- and PTX-insensitive-mediated components equally. Our data suggest that factors promoting RGS2L gene induction may regulate Ca^{2+} influx through L channels by recruiting low-affinity interactions with $G_{i/o}$ that are absent at basal RGS2L levels.

(Received 16 October 2002; accepted after revision 21 February 2003; first published online 21 March 2003)
Corresponding author M. Toselli: Dipartimento di Scienze Fisiologiche e Farmacologiche Cellulari e Molecolari, Universita' di Pavia, Via Forlanini 6, I-27100 Pavia, Italy. Email: mtoselli@unipv.it

The activation of voltage-dependent L-type Ca^{2+} (L) channels transduces electrical stimuli into contraction in smooth and skeletal muscle cells (Tanabe *et al.* 1987; Mikami *et al.* 1989; Takimoto *et al.* 1997; Striessnig, 1999; Platzer *et al.* 2000) and into hormone release in neuroendocrine cells (Ashcroft *et al.* 1994; Barg *et al.* 2001; Safa *et al.* 2001). In neurons, L currents play a significant role in multiple cellular functions including neurotransmitter release (Rane *et al.* 1987; Vedder & Otten, 1991; Evans & Pocock, 1999; Sand *et al.* 2001), regulation of gene expression (Finkbeiner & Greenberg, 1998; Dolmetsch *et al.* 2001; Mermelstein *et al.* 2001), dendritic development (Schwab *et al.* 2001), cell survival (Galli *et al.* 1995; Mao *et al.* 1999; Xia *et al.* 2002) and synaptic plasticity (Weisskopf *et al.* 1999; Thibault *et al.* 2001; Akopian & Walsh, 2002). In addition to voltage and electrical activity, several neurotransmitters, hormones and cytokines activate a variety of signalling pathways to regulate the influx of Ca^{2+} through L channels. Although this modulation has been thoroughly characterized in cardiac and endocrine cells (Kamp & Hell, 2000; Carbone *et al.* 2001), only a few studies have focused on L channel modulation in neurons.

Neurotransmitters inhibit L channels via binding to G-protein-coupled receptors and subsequent activation of $G_{i/o}$ and/or $G_{q/11}$-mediated pathways (Ewald *et al.* 1989; Howe & Surmeier, 1995; Wilk-Blaszczak *et al.* 1996). Recent studies using both native and heterologously expressed channels indicate that L currents do not exhibit the voltage-dependent inhibition that is typical of N- or P/Q-type Ca^{2+} currents (Mathie *et al.* 1992; Bourinet *et al.* 1996; Connor & Henderson, 1997; Bell *et al.* 2001), produced by the direct binding of $G\beta\gamma$ to the channel (Herlitze *et al.* 1996; Ikeda, 1996). Rather, a number of voltage-independent forms of L channel inhibition have been reported, including phospholipase Cβ1 activation-dependent inhibition (mediated by $G_q\beta\gamma$; Howe & Surmeier, 1995; Hernandez-Lopez *et al.* 2000), phospholipase Cβ1-activation-independent inhibition (coupled to $G\alpha_{q/11}$; Bannister *et al.* 2002), $G_{i/o}$-stimulated release of Ca^{2+} from intracellular stores (Kramer *et al.* 1991; Oz *et al.* 1998) or $G_{i/o}$-mediated activation of protein kinase C (McCullough *et al.* 1998). These observations suggest that intracellular molecules capable of modifying G-protein activity may play an important role in regulating Ca^{2+} influx through L channels.

Recently, a novel family of modulators of heterotrimeric G-proteins has been described (Druey *et al.* 1996; Koelle & Horvitz, 1996; De Vries *et al.* 2000; Ross & Wilkie, 2000). Regulators of G-protein-signalling (RGS) proteins rapidly terminate G-protein-coupled signalling by either: (i) accelerating the rate of intrinsic GTP hydrolysis of Gα subunits and promoting the formation of inactive heterotrimers (Berman *et al.* 1996) or (ii) acting as 'effector antagonists' – i.e. binding to Gα subunits and physically blocking their interaction with downstream signalling molecules (Melliti *et al.* 2000, 2001). Among the 20+ members of the RGS family, RGS2 is broadly distributed throughout the nervous system (Ingi *et al.* 1998; Grafstein-Dunn *et al.* 2001) and has been shown to regulate N-type Ca^{2+} channel inhibition and K^+ channel activation by G-proteins in neurons (Herlitze *et al.* 1999; Kammermeier & Ikeda, 1999; Kammermeier *et al.* 2000; Melliti *et al.* 2001). RGS2 can interact with both G-protein types known to inhibit L channels – $G_{q/11}$ and $G_{i/o}$ – with a preference for $G\alpha_{q/11}$ *in vitro* (Heximer *et al.* 1997, 1999).

In this study we tested the ability of a novel RGS2 splice variant from chick dorsal root ganglion (DRG) neurons, RGS2L, to regulate L channel modulation. Experiments were performed in NG108-15 cells, in which L channel inhibition by both $G_{i/o}$ and a PTX-insensitive G-protein (presumably $G\alpha_{q/11}$) has been well documented (Wilk-Blaszczak *et al.* 1996; Connor & Henderson, 1997). These cells do not express RGS2 endogenously, providing the opportunity to study the selectivity of recombinant RGS2L action on these two G-protein pathways. RGS2L reduces both PTX-sensitive and -insensitive bradykinin-induced inhibition of neuronal L channels and accelerates recovery from inhibition. The extent of inhibition of the $G_{i/o}$- *vs.* the PTX-insensitive pathway directly depended on RGS2L intracellular concentrations. Our results suggest that factors inducing RGS2L upregulation may be important determinants of RGS2L selectivity.

METHODS

Materials

Tetrodotoxin (TTX), bradykinin (BK), theophylline, penicillin and prostaglandin E_1 (PGE_1) were purchased from Sigma Chemical Co. (St Louis, MO, USA), pertussis toxin (PTX) from List Biological Laboratories (Campbell, CA, USA) and ω-conotoxin GVIA from Alomone Labs (Jerusalem, Israel). All other chemicals were from Sigma.

Cloning of the RGS core domain of chick RGS2

Dorsal root ganglion neurons were dissected from 11- or 12-day-old chick embryos (Charles River SPAFAS, North Franklin, CT, USA) killed by decapitation, as described previously (Lü & Dunlap, 1999). All procedures were carried out in accordance with the Tufts University animal welfare committee guidelines. Total RNA was extracted by a phenol–guanidinium thiocyanate method (Tel-Test Inc., Friendswood, TX, USA). Freshly obtained RNA (0.5–1 μg) was then used as a template for reverse transcription using Moloney murine leukaemia virus reverse transcriptase (2.5 U μl^{-1}; Perkin-Elmer), 4 mM dNTP mix and a 1:1 mix of random-hexamer and oligo(dT) (2.5 μM) as primers. The reaction mixture was heated at 42 °C for 15 min for first strand synthesis. After addition of 1 U of Taq DNA polymerase (Gibco) and 1 μM each of degenerate sense (5′-GAG AAC ATG(T) C(T)TC (A)TTC TGG-3′) and antisense (5′-TAG(T) GAG TCC CG(T)G TGC AT-3′) primers, PCR was performed using the following cycling protocol: 94 °C for 1 min (1 cycle), 94 °C for 30 s, 45 °C for 1 min, 72 °C for 1 min (40 cycles), 72 °C for 5 min (1 cycle). Reaction products of the expected size (~240 bp) were subcloned into pCR2.1 (Invitrogen), mapped by restriction digestion and sequenced. Seven independent clones yielded identical partial fragments of the RGS core domain from chick RGS2.

Full-length cloning of chick RGS2 splice variants RGS2S and RGS2L by library screening

An embryonic chick DRG cDNA library (in λZAP II vector) was constructed as described previously (Lü & Dunlap, 1999), and contained 1.7×10^6 primary inserts with an average length of 1.55 kb (size-selected at 600 bp). The final titre was 6.1×10^9 plaque-forming units (pfu) ml^{-1}. In each round of screening, about 1 million plaques were plated and transferred to Nytran membranes (Schleicher & Schuell) in duplicate. Phage DNA was denatured (0.5 M NaOH, 1.5 M NaCl) and neutralized (0.5 M Tris-HCl, 1.5 M NaCl, pH 8.0). A 240 bp cDNA probe, corresponding to a fragment of chick RGS2 RGS domain (see above), was labelled with [α-^{32}P]dCTP using a random-priming kit (Amersham Pharmacia Biotech) and added to a hybridization solution of 50 % deionized formamide, 0.8 M NaCl, 20 mM Pipes, 0.5 % SDS and 100 μg ml^{-1} denatured salmon sperm DNA. After hybridization overnight at 42 °C, membranes were washed twice at 58 °C for 45 min in wash buffer (0.1 × saline–sodium citrate buffer (SSC), 0.1 % SDS). Double-positive plaques were isolated, amplified and subjected to a second round of screening. Individual phage positive after the second screening were subjected to *in vitro* excision using the Exassist/SORL system (Stratagene, La Jolla, CA, USA). Each phage gave rise to a phagemid (pBluescript) containing an individual cDNA clone. The presence of a cDNA insert in the phagemid was confirmed by restriction digestion and sequence analysis. The screening yielded two distinct full-length cDNAs.

Northern blot analysis

Twelve-day-old chick embryos were dissected and total RNA was extracted from several tissues as described above. Poly(A)$^+$ RNA samples were then obtained with the Poly(A)$^+$ Tract mRNA Purification System (Promega, Madison, WI, USA). An agarose gel (0.7 % agarose, 2.2 M formaldehyde, 20 mM Mops, 8 mM sodium acetate, 1 mM EDTA, pH 7.0) was loaded with poly(A)$^+$ RNA from each tissue (1.5 μg); following electrophoresis, the RNA was transferred to a Nytran membrane by alkaline transfer (8 mM NaOH, 3 M NaCl, 1.5 h). A 240 bp RGS core domain fragment, common to chick *RGS2S* and *RGS2L*, was labelled with [α-^{32}P]dCTP by random priming (see above), and 1×10^7 d.p.m. ml^{-1} of probe was added to the hybridization solution (NorthernMAX prehyb/hyb buffer, Ambion, Austin, TX, USA). The blot was hybridized overnight at 42 °C and then washed twice (45 min at 60 °C) in NorthernMAX wash buffer (Ambion). After drying, the membranes were analysed by autoradiography.

Expression and purification of recombinant chick RGS2L

A six His tag (His_6) was engineered by PCR at the C-terminus of chick *RGS2L*; the resulting construct was subcloned into the *Nde*I/*Bam* HI sites of pET11a (Novagen), and used to transform

Escherichia coli BL21 (DE3) cells. A 10 ml overnight culture from a single colony was used to inoculate 1 l of Luria-Bertani (LB) medium with ampicillin (100 μg ml^{-1}) at 37 °C. Isopropyl-1-thio-β-D-galactopyranoside (50 μM) induction was performed at an optical density of 600 nm (OD_{600}) = 0.6–0.8, and cell cultures were shaken for 12 h prior to harvest. Cells were then pelleted, resuspended in buffer A (50 mM Hepes, pH 8, 20 mM β-mercaptoethanol, 100 mM NaCl, 0.1 mM phenylmethylsulphonylfluoride) and lysed by addition of lysozyme (0.2 mg ml^{-1}) and sonication. DNase I (5 μg ml^{-1}) was added to reduce viscosity. The resulting lysate was centrifuged (12 000 *g* for 30 min, at 4 °C) and the supernatant was loaded onto a column containing 1 ml of Ni-NTA affinity resin (Qiagen, Hilden, Germany) pre-equilibrated with buffer A. The column was washed with 50 ml of buffer A + 50 mM imidazole and chick RGS2L was eluted with 5 ml of buffer A + 250 mM imidazole. The eluted protein was dialysed overnight against 1 l of buffer B (50 mM Hepes, 2 mM dithiothreitol (DTT), pH 8), concentrated using a Centricon 10 column (Amicon) and stored at −80 °C. RGS2L protein preparations were 80–90 % pure by Coomassie blue staining of conventional SDS-polyacrylamide gels. The presence of the 13 additional N-terminal amino acids that characterized the longer RGS2 splice variant was confirmed by sequencing. Purified, recombinant RGS2L was routinely sequenced to verify its identity before its utilization for electrophysiological recordings.

Cell culture

Rat NG108-15 neuroblastoma × glioma hybrid cells were grown in monolayers in DMEM (Dulbecco's modified Eagle's medium), 10 % heat-inactivated fetal calf serum, HAT (hypoxanthine–aminopterin–thymidine) supplement, 100 μg ml^{-1} streptomycin and 100 i.u. ml^{-1} penicillin in a 5 % CO_2 humidified atmosphere at 37 °C. Cells were grown in plastic flasks and plated on plastic Petri dishes for use in electrophysiological experiments. The culture medium was replaced three times per week.

To induce cell differentiation and Ca^{2+} channel expression (Kasai & Neher, 1992), 10 μM PGE_1 and 1 mM theophylline were added to the culture medium of NG108-15 cells at least 5 days prior to electrophysiological recordings.

Detection of rat RGS2 in NG108-15 cells

Total RNA was extracted by a phenol–guanidinium thiocyanate method (Tel-Test Inc.) from either rat brain or differentiated (see above) NG108-15 neurons. Freshly obtained RNA (0.5–1 μg) was reverse transcribed as described above, then used as a template for PCR after addition of 1 U of Taq DNA polymerase (Gibco) and 1 μM each of either N-terminal sense (5′-ATG CAA AGT GCC ATG TTC CTG GC-3′) and N-terminal antisense (5′-GAG CAG CGC CTT CCT CAG G-3′), or C-terminal sense (5′-GAA GAA AAT ATT GAA TTC TGG TTG GC-3′) and C-teminal antisense (5′-ATA AGA GTT GTT CTC CAT CAG GC-3′) primers. Primer sequences were based on published rat *RGS2* sequences (GenBank accession numbers: AF279918, AF321837, AY043246) and amplified either the first 79 amino acids (aa) of rat RGS2 (N-terminal primers) or aa 108–186 in the highly conserved RGS core domain (C-terminal primers). Primers annealing to aa 99–193 of rat Gα-interacting protein (GAIP; sense: 5′-ACG GGC CGC AGT GTA TTC CGG GC-3′; antisense: 5′-GTA GGA GTC CCG GTG CAT GAG GG-3′) were used as a positive control for the NG108-15 cDNA. The PCR cycling protocol was: 94 °C for 1 min (1 cycle), 94 °C for 30 s, 65 °C for 1 min, 72 °C for 1 min (40 cycles), 72 °C for 5 min (1 cycle). All reaction products were subcloned into pCR2.1 (Invitrogen), and their identity was confirmed by sequencing.

Electrophysiology

For all experiments, the patch pipettes were filled with (mM): 125 CsCl, 20 tetraethylammonium chloride, 10 EGTA, 1 $CaCl_2$, 1 $MgCl_2$, 4 Mg-ATP, 0.1 GTP, 10 Hepes-CsOH (pH 7.4). Seals between electrodes and cells were established in a solution containing (mM): 135 NaCl, 1.8 $CaCl_2$, 1 $MgCl_2$, 5.5 KCl, 10 glucose, 10 Hepes-NaOH (pH 7.4). After establishing the whole-cell configuration, cells were perfused with an external saline containing (mM): 135 NaCl, 10 $CaCl_2$, 1 $MgCl_2$, 10 glucose, 10 Hepes-NaOH (pH 7.4), 1 4-aminopyridine, 10 tetraethylammonium chloride, 10^{-3} TTX. Most differentiated NG108-15 cells expressed low-voltage-activated T-type, and high-voltage-activated L- and N-type Ca^{2+} channels (Tsunoo *et al.* 1986; Kasai & Neher, 1992). L-type currents were isolated by pre-incubating the cells for about 10 min with 0.1 μM ω-conotoxin GVIA, focal perfusion of the tested cells with the same amount of toxin dissolved in the external recording solution to block N-type channels, and holding the membrane potential of the cell at −40 mV to inactivate T-type Ca^{2+} currents. Under these conditions, following further cell perfusion with 5 mM nifedipine to block L-type channels, the residual Ca^{2+} current was negligible (4 ± 3 %, n = 8), demonstrating that 0.1 μM ω-conotoxin GVIA was effective in completely blocking N-type channels. This conclusion was corroborated by the observation that, following application of 0.1 μM ω-conotoxin GVIA, a second application of the toxin at a concentration of 1 μM caused a negligible decrease of the Ca^{2+} current (6 ± 4 %, n = 5). For all experiments, BK was diluted into the extracellular solution to a working concentration of 100 nM, while RGS2L (stored in buffer B, see above) was diluted into the patch pipette solution to a final concentration of either 10 nM or 1 μM, as indicated. External solutions were exchanged using a fast multi-barrel delivery system positioned close to the recorded cells. Whole-cell currents were recorded under voltage clamp at room temperature (20–24 °C) with a List LM/EPC7 patch-clamp amplifier (List Electronic, Darmstadt, Germany), and digitized at sampling intervals of 26–100 μs using a 12 bit A/D Tecmar LabMaster Board interfaced with an Intel 486 computer. Stimulation, acquisition and data analysis were carried out with pClamp (Axon Instruments Inc., Burlingame, CA, USA) and Origin (Microcal Software Inc., Northampton, MA, USA) software. Linear components of leak and capacitative currents were first reduced by analogue circuitry and then cancelled by P/4 subtraction. Patch pipettes were made from borosilicate glass tubing (Hilgenberg GmbH, Malsfeld, Germany) and fire polished to a final resistance of 0.5–2.0 MΩ when filled with the internal solution. Currents were filtered at 3 kHz. The amount of current inhibition by BK was measured as follows: Ca^{2+} currents were evoked by a 50 ms test pulse to +10 mV in the presence or absence of 100 nM BK. Currents were measured at the time that control currents peaked (T_p); modulated currents were obtained by taking the difference at T_p between control and residual currents following BK application and then normalized to control and expressed as a percentage. All data in the text and figures are given as means ± S.E.M. for n observations. Statistical significance (P) was calculated using Student's paired t test. Fitting of the prepulse/postpulse data was performed by a non-linear regression method based on the Levenberg-Marquardt algorithm.

RESULTS

Cloning of chick *RGS2* cDNA

RNA from chick DRG neurons was used as a template for RT-PCR with degenerate primers. The reactions yielded a

240 bp cDNA fragment having 92 % identity to human *RGS2*, which was later used to probe an embryonic chick DRG cDNA library. A small number of positive clones carried a 1517 bp cDNA encoding a putative 212 aa protein, the avian homologue of mammalian RGS2 (Burchett *et al.* 1998; Ingi *et al.* 1998). We called it RGS2S. Most of the positive clones, however, contained a 1463 bp cDNA, coding for a novel, longer RGS2 splice variant. We named the novel protein RGS2L, since it had 13 additional, N-terminal aa when compared with RGS2S and mammalian RGS2 proteins (Fig. 1*A*).

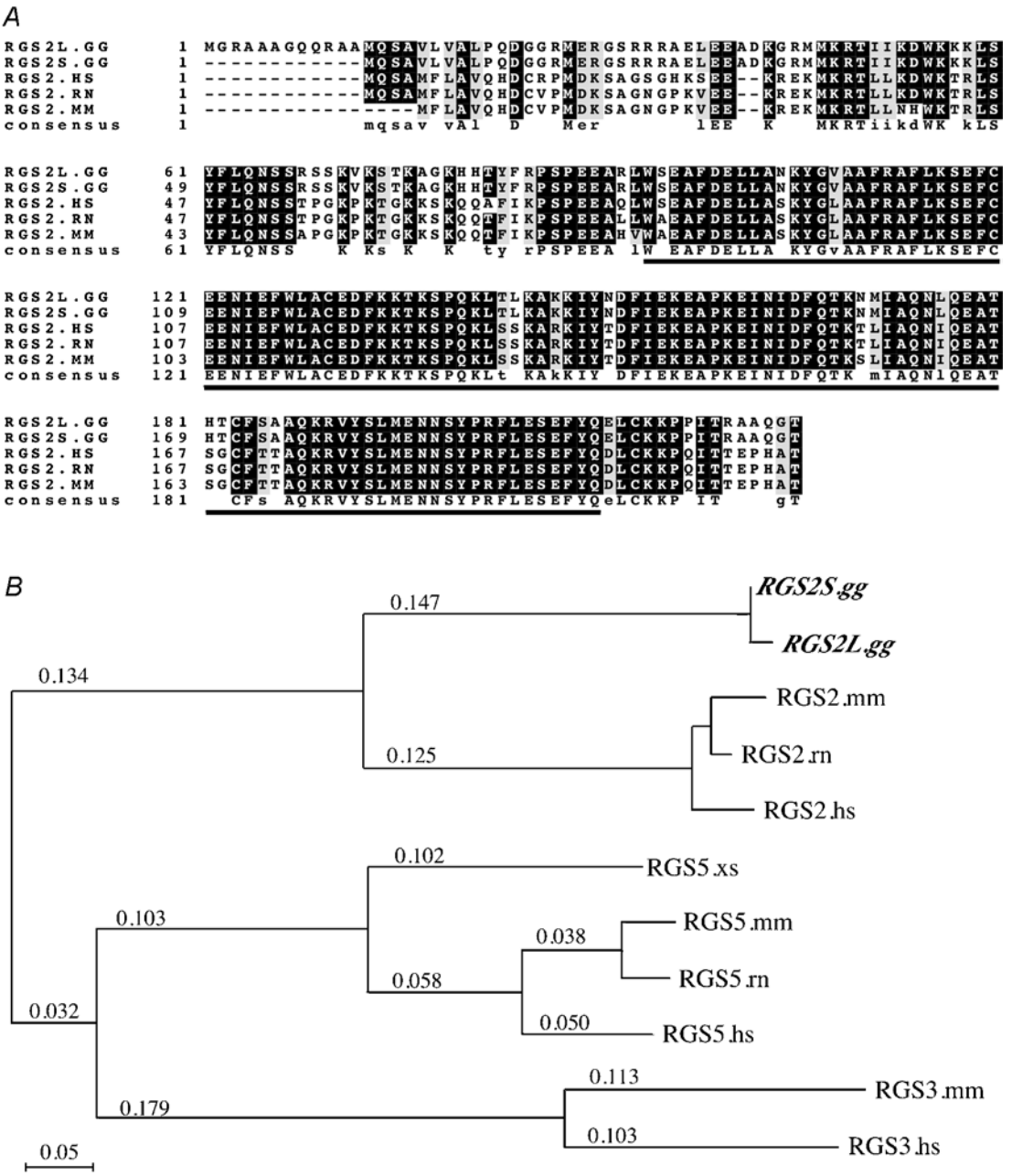

Figure 1. Sequence analysis of chick RGS2S and RGS2L

A, alignment of the predicted amino acid sequences for chick (.GG) RGS2S and RGS2L, and mammalian RGS2 proteins (human, .HS; rat, .RN; mouse, .MM). Identical residues are shaded black; homologous residues are shaded grey. The black bar indicates the RGS domain. Sequences were aligned and shaded using the CLustalX and MacBoxshade programs running locally on a Macintosh G3 PowerPC. *B*, unrooted tree of RGS2, RGS5 and RGS3 family members, generated by neighbour-joining distance methods from the alignment in *A* using the CLustalX program. This tree provides an approximation to the actual evolutionary tree, showing sequence relatedness as a function of branch length, where the branch length is proportional to the amount of change along that branch (sequence distance). Scale bar indicates a 5 % change in amino acid sequence.

Chick *RGS2L* cDNA had a putative translation initiation codon at nucleotide 7, preceded by a satisfactory Kozak's consensus sequence (Kozak, 1987) and a TGA stop codon at nucleotide 682. Analysis of the primary structure of chick *RGS2L* predicts a 225 aa, 25.9 kDa protein. The 3′ untranslated region ends with an uninterrupted sequence of seven adenosines. It contains two TTTGT motifs, thought to play a role in transcriptional activation and present in immediate early genes (Blum *et al.* 1990; Freter *et al.* 1992). This observation suggests that chick *RGS2L* mRNA may be upregulated following specific stimuli, as seen for mammalian *RGS2* mRNAs (Burchett *et al.* 1998; Ingi *et al.* 1998). The coding region contains a 120 aa C-terminal RGS domain, and several putative phosphorylation sites for protein kinase C, protein kinase A, casein kinase II and tyrosine kinase. The presence of a bipartite nuclear localization signal – RRRAELEEADKG RMMKRT – indicates RGS2L as a putative nuclear protein, as reported for mammalian RGS2 (Heximer *et al.* 2001; Song *et al.* 2001). Chick RGS2L also contains a putative N-terminal myristoylation site at position 6.

When a bootstrap tree is built from the chick *RGS2* clones and their eight most related sequences (retrieved with a BLAST similarity search), we observe that the chick proteins branch out with mammalian RGS2 proteins, confirming their identities as *RGS2* gene family members (Fig. 1*B*). In fact, the protein sequences of chick RGS2S and 2L share > 65 % identity with human RGS2. The relatedness to RGS3 and RGS5 proteins (> 50 % identity) further suggests that the chick clones belong to the RGS4 subfamily of RGS proteins (Zheng *et al.* 1999).

Tissue distribution of chick RGS2 mRNAs

A chick poly(A)$^+$ Northern blot was probed with a cDNA fragment encoding a region of the RGS core domain common to chick RGS2L and 2S. Significant hybridization was observed in all chick tissues tested with the exception of brain (Fig. 2, top). A single band of the size of *RGS2L* mRNA was seen in samples from liver and skeletal muscle. In contrast, both *RGS2S* and *RGS2L* overlapping bands were observed in samples from DRG, heart, lung and kidney. In tissues where both *RGS2* variants were present, the two were expressed at comparable levels. In all tissues, a single band was obtained when the blot was stripped and re-hybridized with a probe to the human glyceraldehyde-3-phosphate dehydrogenase (GAPDH) mRNA, a house-keeping gene used as a control for mRNA loading (Fig. 2, bottom).

BK-induced inhibition of L channels is voltage independent and is mediated by both PTX-sensitive and -insensitive G-proteins

In vitro assays have suggested that RGS2 is selective for $G_{q/11}$-mediated pathways (Heximer *et al.* 1997, 1999). Furthermore, the upregulation of mammalian *RGS2* mRNA by a variety of stimuli (Burchett *et al.* 1998; Ingi *et al.* 1998) suggests that the quality and extent of RGS2 effects may depend on its intracellular concentration. We therefore wanted to test the activity of chick RGS2L in a system that: (1) does not have any endogenous RGS2 and (2) has a well-characterized $G_{q/11}$ pathway linked to L channels. Chick DRG neurons are not the ideal preparation as they constitutively express RGS2 proteins and no $G_{q/11}$ pathways have been described for these cells (Boyd *et al.* 1991; Cox & Dunlap, 1992; Cui & Goldstein, 2000; Tata *et al.* 2000). For these reasons, we decided to dialyse purified recombinant, His_6-tagged RGS2L into differentiated rat NG108-15 neurons.

NG108-15 is a well-studied cell line that acquires a neuronal phenotype following *in vitro* differentiation (Hamprecht, 1977). These cells were ideal for our purposes since, when differentiated they do not express any RGS2 isoform, as shown by RT-PCR analysis (Fig. 4*A*). However, they express both neuronal receptors and L-type calcium channels (Kasai & Neher, 1992; Lin *et al.* 1993; Jones & Yakel, 1998; Toselli *et al.* 1999). In particular, these cells possess type-2 BK receptors that inhibit L channels through coupling to both PTX-sensitive $G_{i/o}$ and PTX-resistant $G_{q/11}$ (Wilk-Blaszczak *et al.* 1996; Connor & Henderson, 1997). At 10 mV, bath application of 100 nM BK reversibly reduced L current by 39 ± 2 %, $n = 18$ (Fig. 3*A*). The use of a classical three-pulse protocol (Bean, 1989; Kasai & Neher, 1992) showed that BK-induced inhibition was voltage independent (Fig. 3*B* and *C*). After 24 h incubation with PTX, BK inhibited L channels by 25 ± 4 % ($n = 17$), compared with 39 % in untreated cells. Considering that PTX selectively and irreversibly inactivates $G_{i/o}$ proteins, these data indicate that approximately two-thirds of BK-mediated inhibition of L channels occurs via the PTX-insensitive pathway, while $G_{i/o}$ mediates the remaining third. Both onset and recovery from inhibition were slow ($\tau_{on} = 27 \pm 6$ s, $n = 8$; $\tau_{off} = 229 \pm 18$ s, $n = 8$),

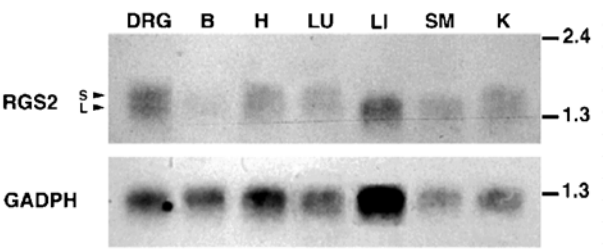

Figure 2. Northern blot analysis of chick *RGS2S* and *RGS2L* mRNAs

Chick poly(A)$^+$ Northern blot, hybridized with ^{32}P-labelled probes specific for either chick *RGS2* (upper panel) or human glyceraldehyde-3-phosphate dehydrogenase (GADPH) mRNA (lower panel, same blot stripped and reprobed as a control for loading). The RGS2 probe hybridized to both *RGS2S* and *RGS2L* mRNAs. Size markers on the right are in kilobases. Arrowheads on the left indicate sizes of the two identified *RGS2* transcripts (upper panel). DRG, dorsal root ganglia; B, brain; H, heart; LU, Lung; LI, liver; SM, skeletal muscle; K, kidney.

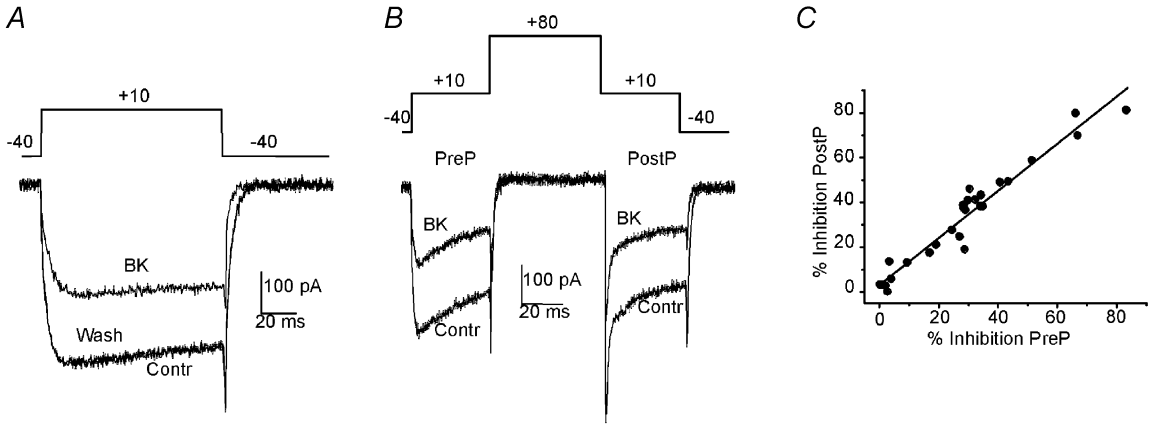

Figure 3. BK-induced inhibition of L channels is voltage independent

A, L currents recorded before (Contr), during (BK) and after (Wash) application of 100 nM BK to an NG108-15 neuron. The voltage protocol is shown above the traces (in mV). *B*, BK-induced inhibition (BK) is not significantly different before (PreP) and after (PostP) application of a 60 ms depolarizing step to +80 mV. The voltage protocol is shown above the traces (in mV). *C*, for each patched cell, BK-mediated inhibition at +10 mV (PreP) is plotted *vs.* the corresponding inhibition measured after the conditioning pulse (PostP). If the inhibition was voltage independent, the slope would be 1. A slope < 1 would indicate a voltage-dependent inhibition (Kammermeier & Ikeda, 1999). The data points are best fitted by a line with a slope of 1.04 ± 0.05 ($n = 27$).

suggesting the involvement of a second messenger cascade rather than a membrane-delimited pathway (Fig. 6*A*). These data are consistent with previously published results (Wilk-Blaszczak *et al.* 1996; Connor & Henderson, 1997).

RGS2L attenuates BK-mediated inhibition of L channels

The effects of chick RGS2L on L channel modulation were investigated by applying recombinant RGS2L intracellularly into NG108-15 neurons via the recording pipette. Therefore, intracellular RGS2L concentration was controlled by the amount of recombinant RGS2L added to the patch pipette solution. Recombinant RGS2L was > 80 % pure as shown by Coomassie blue staining of conventional SDS-PAGE gels (Fig. 4*B*). L currents were measured with 50 ms test pulses to +10 mV and 100 nM BK was applied twice: immediately after break-in (prior to significant RGS2L diffusion) and > 10 min after break-in (after sufficient time for equilibration of RGS2L with the cell interior). This approach allowed: (i) BK-resistant cells

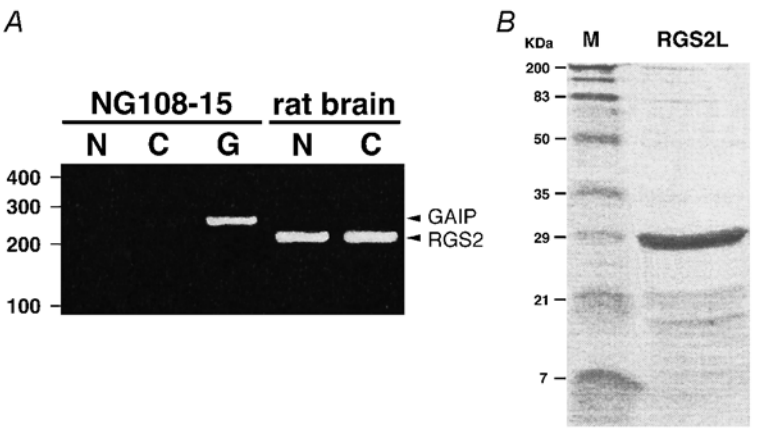

Figure 4. Differentiated NG108-15 cells do not express RGS2

A, RT-PCR was performed on total RNA from differentiated NG108-15 cells and rat brain (positive control). Primer sequences were based on published rat *RGS2* sequences (GenBank accession numbers: AF279918, AF321837 and AY043246; see Methods) and amplified either the first 237 bp (N) or a portion of the highly conserved RGS domain (C) of rat RGS2. No band was amplified in the first two NG108-15 lanes. Primers amplifying the RGS domain of rat GAIP were used as a positive control for the NG108-15 cDNA (G). Arrowheads on the right indicate the expected positions of the RGS2 and GAIP bands. Size markers are shown on the left (base pairs). *B*, the purity of recombinant chick RGS2L preparations was assessed by Coomassie blue staining of conventional SDS-PAGE protein gels. RGS2L preparations were > 80 % pure. Size markers are in the left lane (M).

to be eliminated from the analysis (approximately 15 % of cells tested in this study) and (ii) each cell to be used as its own control. BK-mediated inhibition dramatically decreased following introduction of RGS2L (Fig. 5*A*). After > 10 min exposure to 1 μM RGS2L, BK-mediated inhibition of L current was attenuated by 74 % (10 ± 2 %, compared with 38 ± 3 %, $n = 13$, measured in the same cells immediately after break-in; $P < 0.02$).

To exclude receptor desensitization and washout of intracellular components through the patch pipette as possible causes for the observed RGS2L effects, BK-mediated inhibition was additionally measured in separate populations of control- and RGS2L-dialysed cells > 10 min after break-in. BK-induced inhibition was 67 % smaller in cells perfused with 1 μM RGS2L (11.0 ± 2.2 %, $n = 22$) as compared with cells exposed to control internal solution (33.4 ± 3.0 %, $n = 27$; $P < 0.05$), confirming that RGS2L antagonizes G-protein-mediated inhibition of L current in NG108-15 cells. Interestingly, the attenuation of BK-induced inhibition was dependent on RGS2L concentration (Fig. 5*B*). The BK-mediated inhibition that persisted in the presence of RGS2L remained voltage independent (Fig. 5*C*).

To further exclude non-specific effects of the protein buffer, cells were perfused with boiled RGS2L. In the presence of heat-denatured RGS2L (1 μM), the percentage of BK-mediated inhibition did not significantly differ from that measured without RGS2L (35.1 ± 3.7 %, $n = 6$).

RGS2L accelerates the kinetics of recovery from BK-mediated inhibition

Biochemical evidence indicates that RGS proteins operate as GTPase-activating proteins (GAPs), accelerating Gα-catalysed GTP hydrolysis and controlling the kinetics of G-protein signalling (Berman *et al.* 1996). If the attenuation of BK-mediated inhibition observed for RGS2L-treated cells is due to RGS2L GAP activity, then a change in the rate of recovery from BK-induced inhibition would be expected. To test this, we monitored the time course of recovery from inhibition of L current in control-

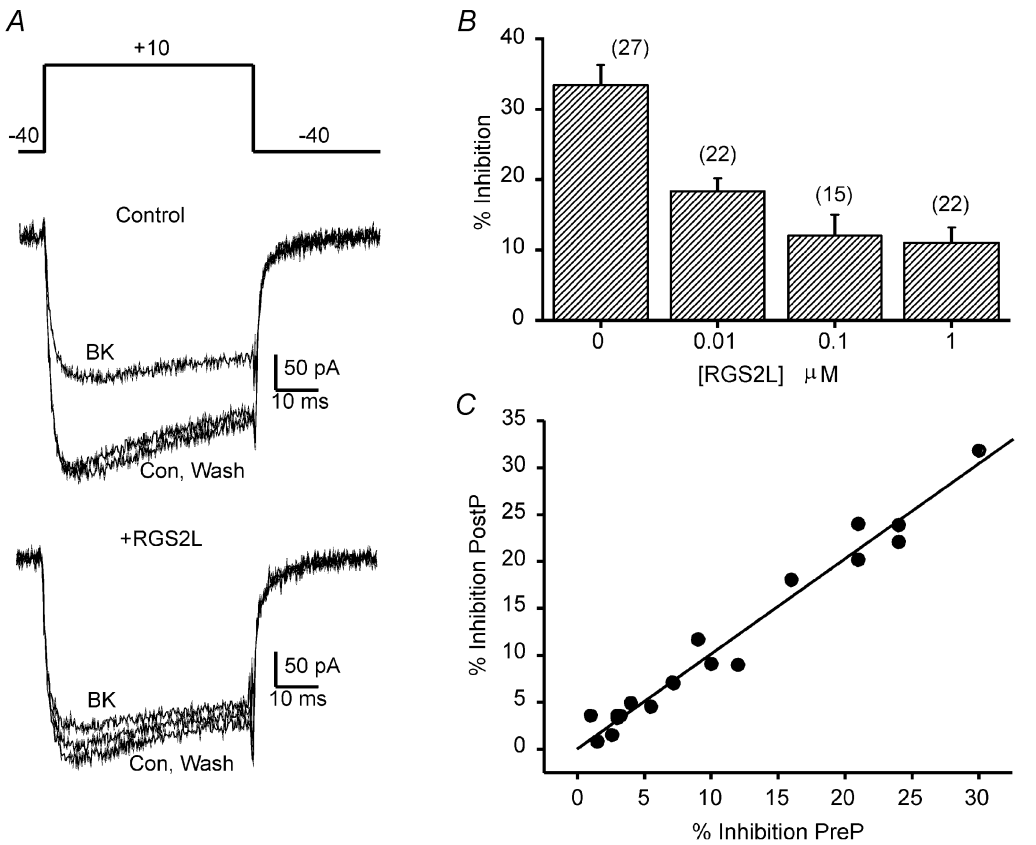

Figure 5. RGS2L attenuates BK-mediated inhibition of L channels

A, L currents recorded from an NG108-15 cell perfused with 1 μM RGS2L, immediately after the whole-cell configuration was achieved (upper traces, Control), and following 15 min RGS2L dialysis (lower traces, +RGS2L). Recordings were made in control saline (Con, Wash) and 100 nM BK. The voltage protocol is shown above the traces. *B*, concentration dependence of RGS2L effects; 1 μM RGS2L is a saturating concentration since it maximally inhibits L channel inhibition. Data in *B* are given as means ± S.E.M. *C*, BK-mediated inhibition is still voltage independent in the presence of RGS2L (1 μM). The PreP *vs.* PostP data points were obtained following cell dialysis for at least 15 min with RGS2L and are all from different cells. They were best fitted by a line with a slope of 1.01 ± 0.04 ($n = 22$).

and RGS2L-perfused cells. Representative data are illustrated in Fig. 6*A*. A 50 ms voltage step to +10 mV was applied at 0.05 Hz before, during and after superfusion of the cell with 100 nM BK. In cells dialysed for > 10 min with control saline, the time courses of onset and recovery from BK-induced inhibition were well described by single exponentials, with average time constants of 29 ± 8 s, ($n = 6$, τ_{on}) and 221 ± 23 s ($n = 6$, τ_{off}), respectively. After intracellular perfusion of 1 μM RGS2, the time constant of onset was similar to control values ($\tau_{on} = 32 \pm 9$ s, $n = 11$, $P > 0.8$). In contrast, the kinetics of recovery from inhibition following BK removal was accelerated by 237 % ($\tau_{off} = 93 \pm 13$ s, $n = 11$, $P < 0.05$; Fig. 6*A* and *B*). A significant acceleration of recovery from inhibition was observed even at a 100-fold lower RGS2L concentration ($\tau_{off} = 79 \pm 3$ s, $n = 7$, $P < 0.05$; Fig. 6*B*). The observed decrease in BK-induced inhibition and the acceleration of the kinetics of recovery from inhibition are consistent with chick RGS2L operating as a GAP and accelerating Gα-catalysed GTP hydrolysis. The unchanged on-rate of inhibition implies that the rate-limiting step is not G-protein activation.

Chick RGS2L specificity towards PTX-insensitive pathways is concentration dependent

RGS2 mRNA is rapidly and transiently upregulated in neurons following a variety of stimuli (Burchett *et al.* 1998; Ingi *et al.* 1998), suggesting that RGS2 protein levels may alter the quality as well as the extent of RGS2 action. The parameter most likely to be influenced by RGS2 concentration is target specificity. In fact, differences in binding affinities for distinct Gα subunits can be compensated for by sufficiently high levels of RGS2 (Heximer *et al.* 1999). *In vitro* studies have shown that human RGS2 interacts preferentially with $G\alpha_{q/11}$ (Heximer *et al.* 1997, 1999). However, it can also bind and modulate $G\alpha_{i/o}$ subunits under certain conditions (Ingi *et al.* 1998; Herlitze *et al.* 1999; Heximer *et al.* 1999). Our goal was to investigate *in vivo* whether: (i) chick RGS2L reduces L current inhibition by acting on a specific G-protein and (ii) changes in RGS2L concentration – such as those occurring during gene induction and protein expression – influence RGS2L activity and target specificity. To this end, we examined the effects of two different concentrations of RGS2L (10 nM and 1 μM) on the PTX-sensitive ($G_{i/o}$-mediated) and PTX-insensitive (probably $G_{q/11}$-mediated) components of BK-induced L current inhibition. The lower RGS2L concentration, 10 nM, is not saturating, while 1 μM RGS2L generates a maximal effect. The PTX-insensitive component was given by the amount of BK-inhibited current in PTX-treated cells. The $G_{i/o}$-dependent inhibition was then estimated by subtracting the PTX-insensitive inhibition from the BK-induced inhibition measured in control cells not treated with PTX (inhibition mediated by both $G_{i/o}$ and the PTX-insensitive component).

After > 10 min dialysis with non-saturating levels of RGS2L (10 nM in the patch pipette), total BK-mediated inhibition of L current was decreased by a total of 45 % (18.3 ± 1.8 %, $n = 22$, $P < 0.05$). Interestingly, the PTX-sensitive and -insensitive components of the inhibition were not equally affected by the RGS protein (Fig. 7*A* and *B*). In fact, 10 nM RGS2L decreased the PTX-insensitive component of L channel inhibition by 57 %, from 21.5 ± 1.8 % ($n = 20$) to 9.3 ± 2.0 % ($n = 23$, $P < 0.05$). In contrast, the $G_{i/o}$-mediated component was reduced by only 24 %, from 11.9 % to 9.0 % (Fig. 7*B*). These

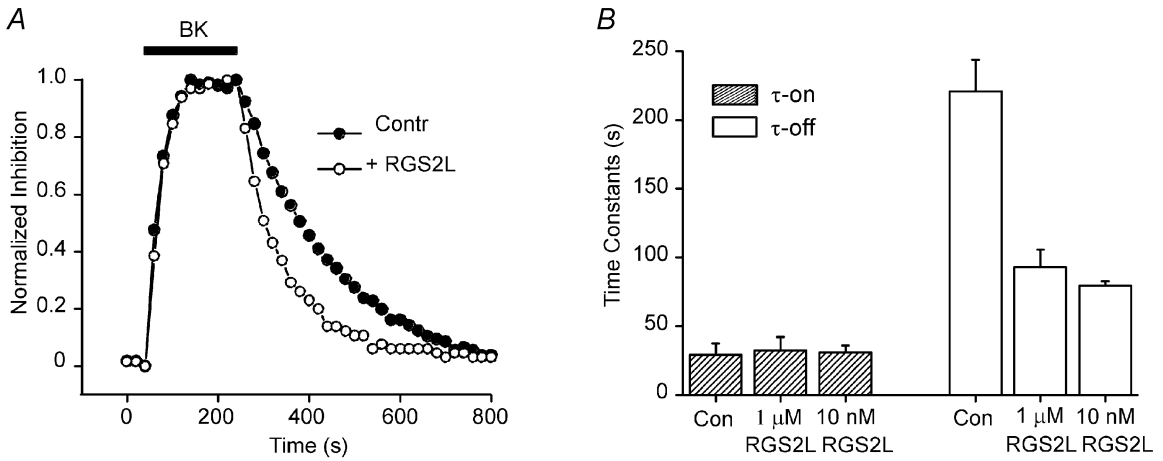

Figure 6. RGS2L accelerates the kinetics of recovery from BK-mediated inhibition

A, BK-mediated inhibition measured every 20 s in a control cell (●) and in a cell perfused with 1 μM RGS2L (○) before, during (BK, bar) and after application of 100 nM BK. To allow comparisons between cells, peak L currents were first transformed into percentages of BK-mediated inhibition (35 and 11 % respectively), then normalized. RGS2L accelerates the recovery from BK-mediated inhibition. *B*, average time constants of onset of (τ-$_{on}$) and recovery from (τ-$_{off}$) BK-mediated inhibition in cells perfused with control saline (Con), 1 μM RGS2L or 10 nM RGS2L. Data in *B* are given as means ± S.E.M.

results indicate that at non-saturating concentrations, chick RGS2L preferentially targets the PTX-insensitive pathway of BK-induced L channel inhibition.

To test the hypothesis that an increase in RGS2L protein levels could affect chick RGS2L activity and target specificity, we studied BK-induced inhibition after dialysis of a 100-fold higher concentration of RGS2L (1 μM in the patch pipette). At saturating concentrations, RGS2L reduced total BK inhibition by 67 % (inhibition was 11.0 % in the presence of RGS2L *vs.* 33.4 % in control-perfused cells, $P < 0.05$, Fig. 7*A*), a 49 % increase in efficacy compared to 10 nM RGS2L. The increased RGS2L efficacy was determined by a stronger inhibition of the $G_{i/o}$ pathway (69 % with 1 μM *vs.* 24 % with 10 nM RGS2L), while the PTX-insensitive pathway was affected approximately equally by these two concentrations (66 *vs.* 57 %, respectively; Fig. 7*B*). These data suggest that the intracellular RGS2L concentration determines the extent of RGS2L activity by modulating the amount of RGS2L–$G_{i/o}$ interaction.

In contrast to results with 10 nM RGS2L, the saturating concentration of RGS2L inhibited the PTX-sensitive and -insensitive pathways equally. In fact, the PTX-insensitive component was reduced by 66 % (from 21.5 ± 1.8 %, $n = 20$ to 7.3 ± 2.5 %, $n = 16$, $P < 0.05$), and the $G_{i/o}$-dependent pathway was reduced by 69 % (from 11.9 % to 3.7 %, Fig. 7*B*). These results show that an increase in intracellular concentration causes RGS2L to lose its relative selectivity for the PTX-insensitive G-protein and suggest that the extent of RGS2L coupling to each pathway varies as a function of intracellular RGS2L concentration.

DISCUSSION

Calcium influx through L channels is an important mechanism through which neurons control dendritic development, gene expression, cellular survival and synaptic plasticity (Rane *et al.* 1987; Finkbeiner & Greenberg, 1998; Weisskopf *et al.* 1999; Schwab *et al.* 2001). Here we show that RGS proteins play a role in L channel modulation. In particular, we have identified a novel RGS2 isoform, RGS2L, which regulates L channel modulation in a concentration-dependent manner.

Chick RGS2L is a novel RGS2 isoform

Chick DRG neurons express two RGS2 isoforms. RGS2S, the shorter of the two, is the exact avian homologue of previously reported human RGS2 (Siderovski *et al.* 1994). RGS2L, on the other hand, is a novel isoform that exhibits 13 additional N-terminal amino acids. The longer N-terminus features a putative myristoylation site that may indicate that RGS2L is preferentially membrane bound.

Chick RGS2L reduces L channel inhibition in a concentration-dependent fashion

Chick RGS2L can modulate L channel inhibition. RGS2L dramatically reduces BK-induced inhibition and accelerates recovery from inhibition on washout of agonist. How does RGS2L function? The most characterized mechanism of

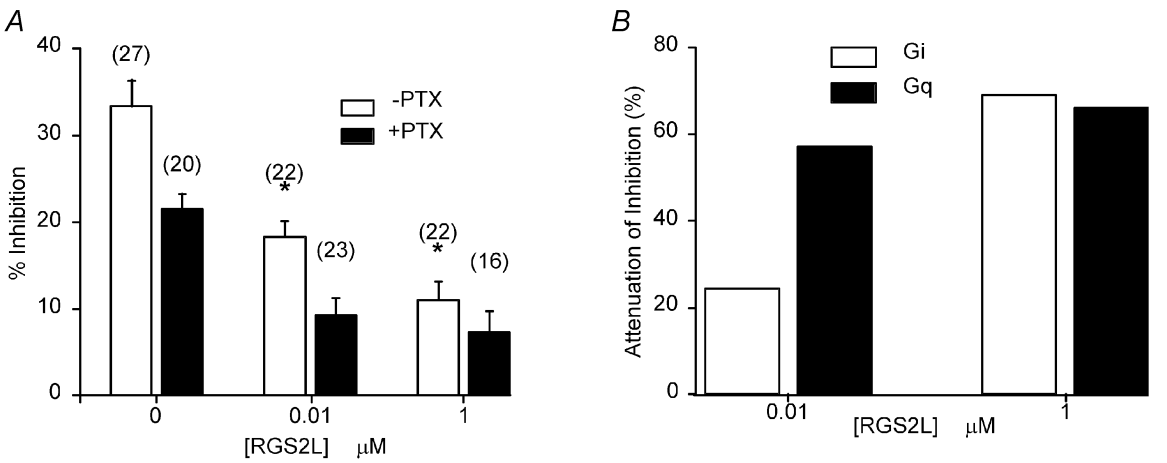

Figure 7. Chick RGS2L specificity is concentration dependent

A, effect of 10 nM and 1 μM RGS2L on BK-induced inhibition in the presence ($G_{q/11}$-mediated, ■) or in the absence ($G_{q/11}$- and $G_{i/o}$-mediated, □) of PTX. Each column is the average of n values (in parentheses). Asterisks indicate values significantly different ($P < 0.05$) from control data, [RGS2L] = 0. Data in *A* are given as means ± S.E.M. *B*, effects of two RGS2L concentrations, 10 nM and 1 μM, on the isolated $G_{i/o}$ (□)- and $G_{q/11}$ (■)-mediated inhibition. Data were inferred from those shown in *A*. The $G_{q/11}$-mediated component was directly obtained from the normalization of the percentage inhibition with and without RGS2L in PTX-treated cells. The $G_{i/o}$-dependent component was then extrapolated by subtraction and normalization of the percentage inhibition between untreated and PTX-treated cells. The $G_{q/11}$-dependent component is maximally reduced by both concentrations, while the $G_{i/o}$-mediated pathway is appreciably inhibited only at saturating RGS2L levels.

action of RGS proteins is their ability to act as GAPs by binding Gα subunits and accelerating their intrinsic GTPase activities (Berman *et al.* 1996; Heximer *et al.* 1997; Ross & Wilkie, 2000). The region responsible for RGS protein GAP activity is the C-terminal, 120 aa RGS core domain (Berman *et al.* 1996). Human RGS2 is a GAP for $G_{q/11}$ and, under certain conditions, for $G_{i/o}$ (Heximer *et al.* 1997; Ingi *et al.* 1998). Human RGS2 and chick RGS2L share > 90 % identity in their RGS core domains, suggesting a strong functional similarity. Indeed, both the observed reduction in BK-induced inhibition and the acceleration of current recovery following BK removal can be entirely explained by RGS2L having GAP activity, which would speed up the termination of the G-protein signal and reduce the concentration of available active subunits. However, under these conditions, RGS2L acting as GAP should also cause an increase in the rate of onset of inhibition, but we did not observe any significant difference from control. An alternative explanation for such RGS effects has recently been proposed (Melliti *et al.* 2000). RGS proteins could bind Gα subunits and act as 'effector antagonists', blocking the interaction of the active Gα subunit with its downstream targets (Melliti *et al.* 2000, 2001; Cunningham *et al.* 2001). This latter mechanism has been observed only for $G_{q/11}$-mediated pathways (Melliti *et al.* 2000). The same RGS protein is capable of both mechanisms of action: human RGS2 inhibits $G_{q/11}$-mediated activation of phospholipase C (PLC)-βt by functioning both as a GAP and as an inhibitor of $G_{q/11}$–PLC-βt interaction (Cunningham *et al.* 2001). Thus, it is possible that RGS2L modulates BK-induced inhibition, at least in part, by acting as an effector antagonist. This hypothesis is supported by the fact that RGS2L does not speed up the kinetics of onset of inhibition, as would be expected if it acted as a GAP.

Previous studies have demonstrated that other neuronal Ca^{2+} channel types can also be regulated by RGS proteins in a fashion similar to that reported here, and recently a block of reconstituted slow muscarinic inhibition of neuronal L-type Ca^{2+} channels by RGS2 and RGS3T has been shown as well (Bannister *et al.* 2002). Endogenous RGS proteins shift the steady-state concentration–response relationship for noradrenaline (norepinephrine)-induced N-type current inhibition to higher concentrations, and dramatically accelerate the current recovery after agonist removal (Jeong & Ikeda, 2000). Similarly, heterologously expressed RGS3, RGS8 and RGS10 decrease G-protein-mediated inhibition of N-type current and accelerate recovery from inhibition in HEK 293 cells (Melliti *et al.* 1999) and in rat superior cervical ganglion neurons (Jeong & Ikeda, 1998). In these studies, RGS proteins act almost entirely through $G_{i/o}$. By contrast, human RGS2 – the RGS protein sharing the highest percentage identity with chick RGS2L – reduces muscarinic inhibition of N- and P/Q-type channels by selectively blocking the $G_{q/11}$-mediated component of the inhibition (Kammermeier *et al.* 2000; Mark *et al.* 2000; Melliti *et al.* 2001).

Target G-protein selectivity is one important determinant of RGS2 function. Human RGS2 preferentially interacts with $G_{q/11}$ pathways both *in vivo* and *in vitro* (Heximer *et al.* 1997, 1999; Bowman *et al.* 1998; Ingi *et al.* 1998; Kammermeier *et al.* 2000). RGS2 selectivity is determined by the geometry of its Gα binding pocket, which is unfavourable to $Gα_{i/o}$ (Heximer *et al.* 1999). Even after artificially raising protein levels through overexpression, RGS2 inhibited $G_{q/11}$ 70 % more efficiently than $G_{i/o}$ *in vivo* (Ingi *et al.* 1998). Since the residues responsible for the specificity of interaction between RGS2 and $G_{q/11}$ are conserved in chick RGS2L (Heximer *et al.* 1999), the two proteins would be expected to exhibit a similar specificity. Surprisingly, chick RGS2L blocked the PTX-sensitive ($G_{i/o}$-mediated) and -insensitive (presumably $G_{q/11}$-mediated) components of BK-induced L channel inhibition equally. It thus appears to be less selective than its human homologue. Several explanations are possible for the reduced specificity. First, RGS2 selectivity may partly depend on poorly conserved residues outside the RGS core domain (the percentage identity between human RGS2 and RGS2L drops to 54 % when the RGS core domain is not considered; Heximer *et al.* 1999). Second, some specificity may be lost when using a chick protein in a rat model. Third, although human RGS2 specificity for $G_{q/11}$ was observed in the presence of artificially elevated RGS2 levels (i.e. cells overexpressing the RGS protein and *in vitro* reconstitution systems; Bowman *et al.* 1998; Ingi *et al.* 1998; Kammermeier *et al.* 2000), intracellular RGS2 concentration was unknown in these studies, and may have been insufficient to promote RGS2 interaction with $G_{i/o}$.

The rapid and transient upregulation of *RGS2* mRNA following a variety of stimuli (Siderovski *et al.* 1994; Burchett *et al.* 1998; Ingi *et al.* 1998; Song *et al.* 2001) suggests that the quality and quantity of RGS2 effects are likely to vary with the physiological state of the cell. Even though the exact intracellular RGS2 concentration at rest and after induction is not known, comparing the effects of a low, non-saturating, and of a high, saturating concentration of RGS2L can provide us with a qualitative prediction of the consequences of RGS2 gene induction. Interestingly, we observed that both the selectivity and efficacy of chick RGS2L depended on its intracellular concentration. These results suggest that RGS2L has a higher binding affinity for the PTX-insensitive G-protein than for $G_{i/o}$, in agreement with results reported for human RGS2 (Heximer *et al.* 1999). It is, thus, anticipated that stimuli inducing RGS2L expression will regulate the extent of RGS2L coupling to the $G_{i/o}$ pathway. This concentration-dependent recruitment of RGS2-mediated $G_{i/o}$ activation would promote a 50 % increase in the efficacy of RGS2.

It is worth noting that even the lower concentration of RGS2L tested produced maximal acceleration in the recovery from inhibition. The further blockade of the $G_{i/o}$ pathway obtained by raising RGS2L concentration to 1 μM had no additional effect on the rate of current recovery. This observation is likely to be due to the fact that both the steady-state rate of hydrolysis (determined by GDP dissociation) and the intrinsic GTPase activity of PTX-insensitive proteins are much slower than those of $G_{i/o}$ (Gilman, 1987; Pang & Sternweis, 1990; Berstein *et al.* 1992), and thus, are likely to be rate limiting. RGS2L-mediated changes in the kinetics of recovery of the $G_{i/o}$ signalling pathways, therefore, would be expected to be negligible compared to the slower $G_{q/11}$-dominated rate.

Functional implications of RGS2L concentration dependence

Our data suggest that RGS2L expression may tightly control G-protein signalling. In cells where RGS2L is upregulated to stimulated levels, both PTX-sensitive and PTX-insensitive pathways are inhibited. By contrast, low, constitutive levels of RGS2L would selectively inhibit the PTX-insensitive pathway without affecting the $G_{i/o}$-mediated pathway. We can speculate that the modulation of intracellular RGS2L concentration by one or more integrated inducing stimuli will determine the type and amount of G-protein inhibited.

RGS2L-mediated reduction of G-protein pathways that target L channels may have consequences for Ca^{2+} homeostasis. Our data indicate that raising RGS2L intracellular concentration will lead to decreased channel inhibition and to increased Ca^{2+} entry. Factors that promote RGS2L gene induction may therefore fine-tune Ca^{2+}-dependent processes such as neurotransmitter release, regulation of gene expression, dendritic development and synaptic plasticity (Rane *et al.* 1987; Finkbeiner & Greenberg, 1998; Weisskopf *et al.* 1999; Schwab *et al.* 2001).

BK is a neuropeptide involved in nociceptive pathways (Dray & Perkins, 1993). BK receptors are localized in the spinal cord, DRG neurons, hypothalamus, thalamus and frontal cortex (Dray & Perkins, 1993). BK excites DRG cells, leading to the sensation of pain (Dray & Perkins, 1993). The abundant expression of RGS2L in DRG neurons (Fig. 2) and its ability to reduce BK-mediated L channel inhibition suggest it may play a role in pain transmission.

In conclusion, we have identified a novel RGS2 splice variant – RGS2L – that is capable of modulating both PTX-sensitive ($G_{i/o}$-mediated) and PTX-insensitive (presumably $G_{q/11}$-mediated) pathways that inhibit L-type calcium channels. Furthermore, we have demonstrated for the first time in a living cell that the extent of RGS2L coupling to each pathway depends on RGS2L intracellular concentration. These results suggest a possible role for factors that stimulate RGS2L gene induction and protein production in the regulation of intracellular Ca^{2+} levels via modulation of L channel inhibition.

REFERENCES

Akopian G & Walsh JP (2002). Corticostriatal paired-pulse potentiation produced by voltage-dependent activation of NMDA receptors and L-type Ca^{2+} channels. *J Neurophysiol* **87**, 157–165.

Ashcroft FM, Proks P, Smith PA, Ammala C, Bokvist K & Rorsman P (1994). Stimulus-secretion coupling in pancreatic beta cells. *J Cell Biochem* **55**, 54–65.

Bannister RA, Melliti K & Adams BA (2002) Reconstituted slow muscarinic inhibition of neuronal ($Ca_V1.2c$) L-type Ca^{2+} channels. *Biophys J* **83**, 3256–3267.

Barg S, Ma X, Eliasson L, Galvanovskis J, Gopel SO, Obermuller S, Platzer J, Renstrom E, Trus M, Atlas D, Striessnig J & Rorsman P (2001). Fast exocytosis with few Ca^{2+} channels in insulin-secreting mouse pancreatic B cells. *Biophys J* **81**, 3308–3323.

Bean BP (1989). Neurotransmitter inhibition of neuronal calcium currents by changes in channel voltage dependence. *Nature* **340**, 153–156.

Bell DC, Butcher AJ, Berrow NS, Page KM, Brust PF, Nesterova A, Stauderman KA, Seabrook GR, Nurnberg B & Dolphin AC (2001). Biophysical properties, pharmacology, and modulation of human, neuronal L-type ($alpha_{1D}$, $Ca_V1.3$) voltage-dependent calcium currents. *J Neurophysiol* **85**, 816–827.

Berman DM, Wilkie TM & Gilman AG (1996). GAIP and RGS4 are GTPase-activating proteins for the Gi subfamily of G protein alpha subunits. *Cell* **86**, 445–452.

Berstein G, Blank JL, Smrcka AV, Higashijima T, Sternweis PC, Exton JH & Ross EM (1992). Reconstitution of agonist-stimulated phosphatidylinositol 4,5-bisphosphate hydrolysis using purified m1 muscarinic receptor, Gq/11, and phospholipase C-beta 1. *J Biol Chem* **267**, 8081–8088.

Blum S, Forsdyke RE & Forsdyke DR (1990). Three human homologs of a murine gene encoding an inhibitor of stem cell proliferation. *DNA Cell Biol* **9**, 589–602.

Bourinet E, Soong TW, Stea A & Snutch TP (1996). Determinants of the G protein-dependent opioid modulation of neuronal calcium channels. *Proc Natl Acad Sci U S A* **93**, 1486–1491.

Bowman EP, Campbell JJ, Druey KM, Scheschonka A, Kehrl JH & Butcher EC (1998). Regulation of chemotactic and proadhesive responses to chemoattractant receptors by RGS (regulator of G-protein signaling) family members. *J Biol Chem* **273**, 28040–28048.

Boyd RT, Jacob MH, McEachern AE, Caron S & Berg DK (1991). Nicotinic acetylcholine receptor mRNA in dorsal root ganglion neurons. *J Neurobiol* **22**, 1–14.

Burchett SA, Volk ML, Bannon MJ & Granneman JG (1998). Regulators of G protein signaling: rapid changes in mRNA abundance in response to amphetamine. *J Neurochem* **70**, 2216–2219.

Carbone E, Carabelli V, Cesetti T, Baldelli P, Hernandez-Guijo JM & Giusta L (2001). G-protein- and cAMP-dependent L-channel gating modulation: a manifold system to control calcium entry in neurosecretory cells. *Pflugers Arch* **442**, 801–813.

Connor M & Henderson G (1997). Bradykinin inhibition of N- and L-type calcium channel currents in NG108-15 cells. *Neuropharmacol* **36**, 115–124.

Cox DH & Dunlap K (1992). Pharmacological discrimination of N-type from L-type calcium current and its selective modulation by transmitters. *J Neurosci* **12**, 906–914.

Cui S & Goldstein RS (2000). Expression of estrogen receptors in the dorsal root ganglia of the chick embryo. *Brain Res* **882**, 236–240.

Cunningham ML, Waldo GL, Hollinger S, Hepler JR & Harden TK (2001). Protein kinase C phosphorylates RGS2 and modulates its capacity for negative regulation of Galpha 11 signaling. *J Biol Chem* **276**, 5438–5444.

De Vries L, Zheng B, Fischer T, Elenko E & Farquhar MG (2000). The regulator of G protein signaling family. *Ann Rev Pharmacol Toxicol* **40**, 235–271.

Dolmetsch RE, Pajvani U, Fife K, Spotts JM & Greenberg ME (2001). Signaling to the nucleus by an L-type calcium channel-calmodulin complex through the MAP kinase pathway. *Science* **294**, 333–339.

Dray A & Perkins M (1993). Bradykinin and inflammatory pain. *Trends Neurosci* **16**, 99–104.

Druey KM, Blumer KJ, Kang VH & Kehrl JH (1996). Inhibition of G-protein-mediated MAP kinase activation by a new mammalian gene family. *Nature* **379**, 742–746.

Evans GJ & Pocock JM (1999). Modulation of neurotransmitter release by dihydropyridine-sensitive calcium channels involves tyrosine phosphorylation. *Eur J Neurosci* **11**, 279–292.

Ewald DA, Pang IH, Sternweis PC & Miller RJ (1989). Differential G protein-mediated coupling of neurotransmitter receptors to Ca^{2+} channels in rat dorsal root ganglion neurons *in vitro*. *Neuron* **2**, 1185–1193.

Finkbeiner S & Greenberg ME (1998). Ca^{2+} channel-regulated neuronal gene expression. *J Neurobiol* **37**, 171–189.

Freter RR, Irminger JC, Porter JA, Jones SD & Stiles CD (1992). A novel 7-nucleotide motif located in 3′ untranslated sequences of the immediate-early gene set mediates platelet-derived growth factor induction of the JE gene. *Mol Cell Biol* **12**, 5288–5300.

Galli C, Meucci O, Scorziello A, Werge TM, Calissano P & Schettini G (1995). Apoptosis in cerebellar granule cells is blocked by high KCl, forskolin, and IGF-1 through distinct mechanisms of action: the involvement of intracellular calcium and RNA synthesis. *J Neurosci* **15**, 1172–1179.

Gilman AG (1987). G proteins: transducers of receptor-generated signals. *Ann Rev Biochem* **56**, 615–649.

Grafstein-Dunn E, Young KH, Cockett MI & Khawaja XZ (2001). Regional distribution of regulators of G-protein signaling (RGS) 1, 2, 13, 14, 16, and GAIP messenger ribonucleic acids by *in situ* hybridization in rat brain. *Brain Res Mol Brain Res* **88**, 113–123.

Hamprecht B (1977). Structural, electrophysiological, biochemical, and pharmacological properties of neuroblastoma-glioma cell hybrids in cell culture. *Int Rev Cytol* **49**, 99–170.

Herlitze S, Garcia DE, Mackie K, Hille B, Scheuer T & Catterall WA (1996). Modulation of Ca^{2+} channels by G-protein beta gamma subunits. *Nature* **380**, 258–262.

Herlitze S, Ruppersberg JP & Mark MD (1999). New roles for RGS2, 5 and 8 on the ratio-dependent modulation of recombinant GIRK channels expressed in *Xenopus* oocytes. *J Physiol* **517**, 341–352.

Hernandez-Lopez S, Tkatch T, Perez-Garci E, Galarraga E, Bargas J, Hamm H & Surmeier DJ (2000). D2 dopamine receptors in striatal medium spiny neurons reduce L-type Ca^{2+} currents and excitability via a novel PLCβ1-IP3-calcineurin-signaling cascade. *J Neurosci* **20**, 8987–8995.

Heximer SP, Lim H, Bernard JL & Blumer KJ (2001). Mechanisms governing subcellular localization and function of human rgs2. *J Biol Chem* **276**, 14195–14203.

Heximer SP, Srinivasa SP, Bernstein, LS, Bernard JL, Linder ME, Hepler JR & Blumer KJ (1999). G protein selectivity is a determinant of RGS2 function. *J Biol Chem* **274**, 34253–34259.

Heximer SP, Watson N, Linder ME, Blumer KJ & Hepler JR (1997). RGS2/G0S8 is a selective inhibitor of Gqalpha function. *Proc Natl Acad Sci U S A* **94**, 14389–14393.

Howe AR & Surmeier DJ (1995). Muscarinic receptors modulate N-, P-, and L-type Ca^{2+} currents in rat striatal neurons through parallel pathways. *J Neurosci* **15**, 458–469.

Ikeda SR (1996). Voltage-dependent modulation of N-type calcium channels by G-protein beta gamma subunits. *Nature* **380**, 255–258.

Ing T, Krumins AM, Chidiac P, Brothers GM, Chung S, Snow BE, Barnes CA, Lanahan AA, Siderovski DP, Ross EM, Gilman AG & Worley PF (1998). Dynamic regulation of RGS2 suggests a novel mechanism in G-protein signaling and neuronal plasticity. *J Neurosci* **18**, 7178–7188.

Jeong SW & Ikeda SR (1998). G protein alpha subunit G alpha z couples neurotransmitter receptors to ion channels in sympathetic neurons. *Neuron* **21**, 1201–1212.

Jeong SW & Ikeda SR (2000). Endogenous regulator of G-protein signaling proteins modify N-type calcium channel modulation in rat sympathetic neurons. *J Neurosci* **20**, 4489–4496.

Jones S & Yakel JL (1998). Ca^{2+} influx through voltage-gated Ca^{2+} channels regulates 5-HT3 receptor channel desensitization in rat glioma × mouse neuroblastoma hybrid NG108-15 cells. *J Physiol* **510**, 361–370.

Kammermeier PJ & Ikeda SR (1999). Expression of RGS2 alters the coupling of metabotropic glutamate receptor 1a to M-type K^+ and N-type Ca^{2+} channels. *Neuron* **22**, 819–829.

Kammermeier PJ, Ruiz-Velasco V & Ikeda SR (2000). A voltage-independent calcium current inhibitory pathway activated by muscarinic agonists in rat sympathetic neurons requires both Galpha q/11 and Gbeta gamma. *J Neurosci* **20**, 5623–5629.

Kamp TJ & Hell JW (2000). Regulation of cardiac L-type calcium channels by protein kinase A and protein kinase C. *Circ Res* **87**, 1095–1102.

Kasai H & Neher E (1992). Dihydropyridine-sensitive and omega-conotoxin-sensitive calcium channels in a mammalian neuroblastoma–glioma cell line. *J Physiol* **448**, 161–188.

Koelle MR & Horvitz HR (1996). EGL-10 regulates G protein signaling in the *C. elegans* nervous system and shares a conserved domain with many mammalian proteins. *Cell* **84**, 115–125.

Kozak M (1987). An analysis of 5′-noncoding sequences from 699 vertebrate messenger RNAs. *Nucleic Acids Res* **15**, 8125–8148.

Kramer RH, Kaczmarek LK & Levitan ES (1991). Neuropeptide inhibition of voltage-gated calcium channels mediated by mobilization of intracellular calcium. *Neuron* **6**, 557–563.

Lin TA, Lustig KD, Sportiello MG, Weisman GA & Sun GY (1993). Signal transduction pathways coupled to a P2U receptor in neuroblastoma x glioma (NG108-15) cells. *J Neurochem* **60**, 1115–1125.

Lü Q & Dunlap K (1999). Cloning and functional expression of novel N-type Ca^{2+} channel variants. *J Biol Chem* **274**, 34566–34575.

McCullough LA, Egan TM & Westfall TC (1998). Neuropeptide Y inhibition of calcium channels in PC-12 pheochromocytoma cells. *Am J Physiol Cell Physiol* **274**, C1290–1297.

Mao Z, Bonni A, Xia F, Nadal-Vicens M & Greenberg ME (1999). Neuronal activity-dependent cell survival mediated by transcription factor MEF2. *Science* **286**, 785–790.

Mark MD, Wittemann S & Herlitze S (2000). G protein modulation of recombinant P/Q-type calcium channels by regulators of G protein signalling proteins. *J Physiol* **528**, 65–77.

Mathie A, Bernheim L & Hille B (1992). Inhibition of N- and L-type calcium channels by muscarinic receptor activation in rat sympathetic neurons. *Neuron* **8**, 907–914.

Melliti K, Meza U & Adams B (2000). Muscarinic stimulation of alpha1E Ca channels is selectively blocked by the effector antagonist function of RGS2 and phospholipase C-beta1. *J Neurosci* **20**, 7167–7173.

Melliti K, Meza U & Adams BA (2001). RGS2 blocks slow muscarinic inhibition of N-type Ca^{2+} channels reconstituted in a human cell line. *J Physiol* **532**, 337–347.

Melliti K, Meza U, Fisher R & Adams B (1999). Regulators of G protein signaling attenuate the G protein-mediated inhibition of N-type Ca channels. *J Gen Physiol* **113**, 97–110.

Mermelstein PG, Deisseroth K, Dasgupta N, Isaksen AL & Tsien RW (2001). Calmodulin priming: nuclear translocation of a calmodulin complex and the memory of prior neuronal activity. *Proc Natl Acad Sci U S A* **98**, 15342–15347.

Mikami A, Imoto K, Tanabe T, Niidome T, Mori Y, Takeshima H, Narumiya S & Numa S (1989). Primary structure and functional expression of the cardiac dihydropyridine-sensitive calcium channel. *Nature* **340**, 230–233.

Oz M, Melia MT, Soldatov NM, Abernethy DR & Morad M (1998). Functional coupling of human L-type Ca^{2+} channels and angiotensin AT1A receptors coexpressed in *Xenopus laevis* oocytes: involvement of the carboxyl-terminal Ca^{2+} sensors. *Mol Pharmacol* **54**, 1106–1112.

Pang IH & Sternweis PC (1990). Purification of unique alpha subunits of GTP-binding regulatory proteins (G proteins) by affinity chromatography with immobilized beta gamma subunits. *J Biol Chem* **265**, 18707–18712.

Platzer J, Engel J, Schrott-Fischer A, Stephan K, Bova S, Chen H, Zheng H & Striessnig J (2000). Congenital deafness and sinoatrial node dysfunction in mice lacking class D L-type Ca^{2+} channels. *Cell* **102**, 89–97.

Rane SG, Holz GGT & Dunlap K (1987). Dihydropyridine inhibition of neuronal calcium current and substance P release. *Pflugers Arch* **409**, 361–366.

Ross EM & Wilkie TM (2000). GTPase-activating proteins for heterotrimeric G proteins: regulators of G protein signaling (RGS) and RGS-like proteins. *Ann Rev Biochem* **69**, 795–827.

Safa P, Boulter J & Hales TG (2001). Functional properties of Cav1.3 (alpha1D) L-type Ca^{2+} channel splice variants expressed by rat brain and neuroendocrine GH3 cells. *J Biol Chem* **276**, 38727–38737.

Sand O, Chen BM & Grinnell AD (2001). Contribution of L-type Ca^{2+} channels to evoked transmitter release in cultured *Xenopus* nerve–muscle synapses. *J Physiol* **536**, 21–33.

Schwab Y, Mouton J, Chasserot-Golaz S, Marty I, Maulet Y & Jover E (2001). Calcium-dependent translocation of synaptotagmin to the plasma membrane in the dendrites of developing neurones. *Brain Res Mol Brain Res* **96**, 1–13.

Siderovski DP, Heximer SP & Forsdyke DR (1994). A human gene encoding a putative basic helix-loop-helix phosphoprotein whose mRNA increases rapidly in cycloheximide-treated blood mononuclear cells. *DNA Cell Biol* **13**, 125–147.

Song L, Zmijewski JW & Jope RS (2001). RGS2: regulation of expression and nuclear localization. *Biochem Biophys Res Commun* **283**, 102–106.

Striessnig J (1999). Pharmacology, structure and function of cardiac L-type Ca^{2+} channels. *Cell Physiol Biochem* **9**, 242–269.

Takimoto K, Li D, Nerbonne JM & Levitan ES (1997). Distribution, splicing and glucocorticoid-induced expression of cardiac alpha 1C and alpha 1D voltage-gated Ca^{2+} channel mRNAs. *J Mol Cell Cardiol* **29**, 3035–3042.

Tanabe T, Takeshima H, Mikami A, Flockerzi V, Takahashi H, Kangawa K, Kojima M, Matsuo H, Hirose T & Numa S (1987). Primary structure of the receptor for calcium channel blockers from skeletal muscle. *Nature* **328**, 313–318.

Tata AM, Vilaro MT & Mengod G (2000). Muscarinic receptor subtypes expression in rat and chick dorsal root ganglia. *Brain Res Mol Brain Res* **82**, 1–10.

Thibault O, Hadley R & Landfield PW (2001). Elevated postsynaptic $[Ca^{2+}]_i$ and L-type calcium channel activity in aged hippocampal neurons: relationship to impaired synaptic plasticity. *J Neurosci* **21**, 9744–9756.

Toselli M, Tosetti P & Taglietti V (1999). Kinetic study of N-type calcium current modulation by delta-opioid receptor activation in the mammalian cell line NG108-15. *Biophys J* **76**, 2560–2574.

Tsunoo A, Yoshii M & Narahashi T (1986). Block of calcium channels by enkephalin and somatostatin in neuroblastoma-glioma hybrid NG108-15 cells. *Proc Natl Acad Sci U S A* **83**, 9832–9836.

Vedder H & Otten U (1991). Biosynthesis and release of tachykinins from rat sensory neurons in culture. *J Neurosci Res* **30**, 288–299.

Weisskopf MG, Bauer EP & LeDoux JE (1999). L-type voltage-gated calcium channels mediate NMDA-independent associative long-term potentiation at thalamic input synapses to the amygdala. *J Neurosci* **19**, 10512–10519.

Wilk-Blaszczak MA, Singer WD & Belardetti F (1996). Three distinct G protein pathways mediate inhibition of neuronal calcium current by bradykinin. *J Neurophysiol* **76**, 3559–3562.

Xia S, Lampe PA, Deshmukh M, Yang A, Brown BS, Rothman SM, Johnson EM Jr & Yu SP (2002). Multiple channel interactions explain the protection of sympathetic neurons from apoptosis induced by nerve growth factor deprivation. *J Neurosci* **22**, 114–122.

Zheng B, De Vries L & Gist Farquhar M (1999). Divergence of RGS proteins: evidence for the existence of six mammalian RGS subfamilies. *Trends Biochem Sci* **24**, 411–414.

Acknowledgements

This work was supported by grants from MIUR (FIRB and COFIN2002) and INFM (to M.T.), a National Institutes of Health grant NS 16483 (to K.D.) and a Human Frontier Science Program Long-Term Fellowship (to P.T.). We wish to thank Dr Q. Lü for assistance with library screening and Northern blots, and all members of the Dunlap laboratory for helpful discussion. The nucleotide sequences reported in this paper have been submitted to the GenBank/EBI database with accession numbers AF502148 and AF502149.

Author's present address

P. Tosetti: INMED/INSERM U29, 163 Avenue de Luminy, BP 13, 13273 Marseille Cedex 09, France.